A Practical Access Point Deployment Optimization Strategy In Communication-based Train Control Systems

Wen, Tao; Constantinou, Costas; Chen, Lei; Li, Zhu; Roberts, Clive

DOI:
10.1109/TITS.2018.2873377

Document Version
Peer reviewed version

Citation for published version (Harvard):
Wen, T, Constantinou, C, Chen, L, Li, Z & Roberts, C 2019, 'A Practical Access Point Deployment Optimization Strategy In Communication-based Train Control Systems', *IEEE Transactions on Intelligent Transportation Systems* , vol. 20, no. 8, pp. 3156-3167. https://doi.org/10.1109/TITS.2018.2873377

A Practical Access Point Deployment Optimization Strategy In Communication-Based Train Control Systems

Tao Wen, Costas Constantinou, Lei Chen, Zhu Li and Clive Roberts

***Abstract*—Communication-based train control (CBTC) systems have been playing a progressively significant role in metro signalling in recent years. As safety-critical systems, CBTC systems have very strict requirements on the wireless communication performance between train and wayside access points (AP), which is highly dependent on the deployment of the APs. In this paper, by customizing and adopting a decomposition-based multiobjective evolutionary algorithm, the proposed AP deployment optimization method has been implemented, verified and its implementation accuracy has been assessed. A real-world case study is carried out in an integrated simulation platform, in which the optimized AP deployments are verified and show better performance than the original planning.**

***Index Terms*—Communication-based train control (CBTC), AP deployment planning, multiobjective optimisation and integrated simulation platform.**

I. Introduction

The world is experiencing huge economic growth, fast urbanization and continuing population increase, especially in some emerging economies. Consequently, the demand for a safer, more efficient and comfortable public mass transit system is becoming more and more urgent [1]. In terms of capacity, safety and reliability, metro systems have been adopted as an ideal option that can meet these urgent demands. As a critical safety system, the main function of a train control system is to avoid potential collisions when trains are running over the network [2]. To redeem this principle, the location of each train on the track must be known by the train control system [3].

Traditionally, track circuits are used to detect the location of trains, the whole track is discretized into many blocks. Once a train enters a block, other trains will not be authorized to do the same. By using this scheme the location of each train can be monitored and potential collisions prevented, but the downside is that exact location detection is impossible to achieve, which affects the scheduling efficiency of metro systems. To overcome this shortcoming caused by the low detection resolution, an increasing number of metro systems tend to use new generation train control systems, which are known as communication-based train control (CBTC) systems. As a modern successor to track circuit-based train control systems, by utilizing the wireless local area network (WLAN), CBTC systems enable timely bi-directional wireless communication between trains and the zone controller (ZC) via associated wayside access points (AP). This technology allows the exact location of each train to be found. In addition, other relevant operational data can be updated with the ZC in real time, and in return, the moving authorities (MA) will be generated by ZC and delivered to relevant trains in a timely fashion.

In a typical CBTC system, the data communication system (DCS) is in charge of building the bi-directional train-to-wayside communications [4]. The brief structure of the DCS in CBTC systems is sketched in outline in Figure 1. The track is divided into different zones and controlled by relevant ZCs. In each zone, a number of APs are allocated and connected with the corresponding ZC via backbone networks; when the train runs within this radio coverage of an AP, bi-directional train-to-wayside communication takes place; when the train leaves this coverage and moves to the next one, a hand-off procedure will be triggered. To achieve continuous bi-directional data exchange, the AP deployment must be sufficiently overlapping. However, a too dense deployment could result in more serious co-channel interference, lower communication system capacity and a higher cost; one the other hand, a minimised spatial overlap could cause radio coverage discontinuities. The deployment of APs is a very important planning issue not only because it determines the overall communication performance, in terms of reliability and capacity, but it can also significantly affect the cost of the train control systems. As stated in a report [5], in mainline railways, the cost of the wireless network takes 40% of the whole budget of building a train control system, which requires over $50,000 per kilometer to construct. However, what is surprising is that about 40% of the wireless network in mainline railways could be wasteful [6]. Even though there is no revealed figures for metro systems, it is easy to imagine that there is an enormous potential in financial cost saving if a more reasonable AP deployment is employed in the DCS. As a result, a well-planned AP deployment is vital for a reliable and cost-effective DCS.

Much research has been conducted towards the optimal placement problem of AP or base stations (BS). In [6], the placement planning problem of BS in the global system for mobile communications for railway (GSM-R) has been addressed, and an optimized BS deployment arrangement is proposed. However, as the network in [6] is assumed to be noise-limited and no interference is taken into account, this method is not suitable for metro systems. More existing work focus on non-railway systems. In [7], an unique framework

The authors are with the Department of Electronic, Electrical and Systems Engineering, University of Birmingham, Birmingham B15 2TT, U.K. The corresponding author is Tao Wen (e-mail: t.wen.uk@outlook.com).

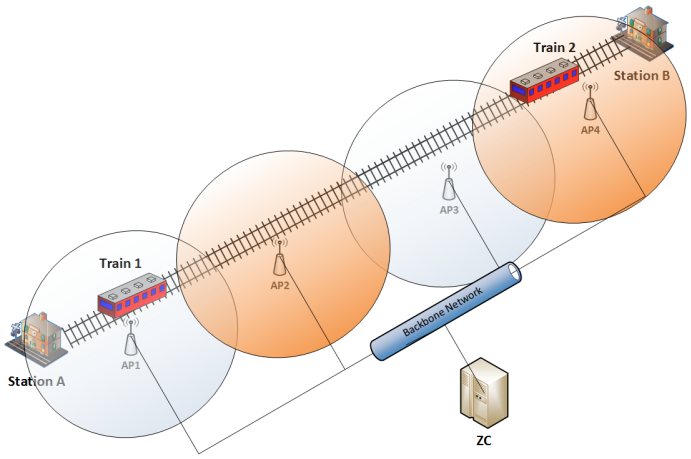

Fig. 1: A diagram of a communication-based train control (CBTC) system

for forming an automatic optimisation tool towards solving the BS placement problem in code-division multiple access (CDMA) based systems is proposed, which contains various BS deployment scenario models and the corresponding customised optimization algorithms. In [8] and [9], a new methodology is proposed to efficiently search an optimal BS deployment scenario for indoor CDMA systems, and a number of potential BS sites and mobile locations are configured by using the brute force search (BFS) algorithm. All the possible up and down-links between BS and mobile will be evaluated, the optimal BS deployment being a subset of these potential BS sites. All prior work focuses on CDMA-based systems, which are not typically used in WLAN systems. As most WLAN systems use orthogonal frequency-division multiplexing (OFDM), to explore the capability of the CDMA-based AP or BS deployment planning methods in the OFDM-based WLAN systems, in [10] some comparisons have been done: By setting the same AP deployment in both OFDM and DS-CDMA based systems, the difference in radio coverage is found, demonstrating that the capability of CDMA-based AP deployment planning methods is not suited to OFDM-based WLAN systems. In [11]–[13], algorithms for AP planning in WLAN systems have been proposed, these being good examples which can be potentially adopted to DCS in CBTC systems. However, as there is no consideration taken of the impact caused by a CBTC-specific environment, there will be underlying uncertainties in the planning result. To achieve a higher efficiency in placement optimization, a new novel optimization method using binary integer programming was proposed in [14], which proposes a new method for solving the AP deployment optimization problem.

By consolidating and extending the existing radio propagation models [15], [16] and [17], and considering the experiments conducted under a railway-specific environment [18], [3] and [19], an AP deployment optimization method for CBTC systems was proposed in our prior work [20]. However, only brute-force exhaustive search was implemented in [20], which is computationally infeasible in planning large-scale DCS systems. Therefore, we have a strong motivation to further extend our prior work. The contributions of this paper will be:

1) Instead of exhaustive search, a more advanced search algorithm, known as the multiobjective evolutionary algorithm based on decomposition (MOEA/D) [21], is introduced and adapted to improve the searching efficiency.
2) An adaptive fading parameter setting subjected to the train location and tunnel dimension is taken.
3) A case study based on a real-world metro line is carried out to illustrate the practicality of the extended optimization methodology.
4) The optimization result is validated in an integrated simulation platform. By comparing the optimised AP deployment communication performance with the original non-optimised AP planning, the achieved improvement is quantified.

The remainder of this paper is arranged as follows: Section II builds dedicated wireless channel models in metro environments, and some simplifying approximation methods for computing the outage probability are investigated. In Section III, the methodology for AP deployment optimization is presented, and an advanced search algorithm, MOEA/D, is customized to our problem. In Section IV, a real-world case study is carried out. In Section V, an integrated test platform is introduced, and the optimized AP deployments are tested to compare with the original planning. Finally, conclusion and future work are presented in Section VI.

II. Channel Modelling

At the physical layer a reliable wireless connection mainly depends on the following factors: path-loss including shadowing (known as large-scale fading), multipath effects (or small-scale fading), the Doppler shift and co-&adjacent-channel interference [22]. Since most WLANs in DCS utilize advanced modulation technologies, such as OFDM and spread spectrum (e.g. frequency-hopping spread spectrum (FHSS)), the impact of multipath effects can be significantly mitigated. As the train speed in metro systems is relatively low (the operational speed is around 60 km/h), the Doppler shift is not significant. Therefore, multi-path effects and the Doppler shift are small and consequently they will be ignored in this paper, which only consider the path-loss plus shadowing. Interference is also considered throughout.

A. Path-loss and Shadowing

When a radiowave is propagating between the train and APs, the power density of the wireless signal suffers a reduction with increasing train-AP separation, which is expressed as [23]:

$$L_{PL}(d)\,[\mathrm{dBm}] = P_t - P_r = 10n\log_{10}(\frac{d}{d_0}) - 10\log_{10}K \tag{1}$$

where L_{PL} is the path-loss; P_t and P_r are the transmitted signal power and the average received signal power in dBm respectively; n is the path-loss exponent, which is subject to

the propagation environment; K is an dimensionless constant that is dependent on the antenna characteristics other than maximum gain, and is subsumed into the path-loss at a reference distance d_0 [24]; and d is the distance between the train and the associated AP in m.

However, in reality, some large obstacles may be located on the propagation path between the transmitter and receiver; these obstacles can obscure the radiowave and cause variation of signal power density, which is referred as shadowing. As a result, the path-loss will be rewritten as:

$$L_{PL}(d)\,[\mathrm{dBm}] = 10n\log_{10}(\frac{d}{d_0}) - 10\log_{10}K - x_{\mathrm{dB}} \quad (2)$$

where x_{dB} represents the signal power density change caused by shadowing, and obeys log-normal distribution $N(\mu_{\mathrm{dB}}, \sigma^2_{\mathrm{dB}})$ [25] where σ_{dB} is the signal strength standard deviation in dB, and μ_{dB} is the mean power of the reviewed signal in dB.

Therefore, by combining path-loss and shadowing effects, the received power is,

$$P_r(d)\,[\mathrm{dBm}] = P_t - 10n\log_{10}(\frac{d}{d_0}) + 10\log_{10}K + G_{tx} + G_{rx} - x_{\mathrm{dB}} \quad (3)$$

where G_{tx} and G_{tx} are the transmitting gain and receiving gain respectively; without counting x_{dB}, the P_r will be the received mean power.

B. Outage Probability and Its Approximation

To meet the requirements of DCS for reliable wireless connection, the received power strength of the desired signal must be higher than the Rx sensitivity. However, owing to shadowing fading, the power density of any radio signal undergoes a random spatial attenuation, and we make use of a complex ray-tracing method or a full-wave propagation prediction method incurring a prohibitively expensive computational overhead, it is almost impossible to predict the exact signal strength at a certain distance. As the shadowing follows a log-normal distribution, we can employ a probability to quantify the likelihood of radio link outage at each spatial location. This probability is referred to as outage probability.

In WLANs, there are two typical scenarios, which are having a noise-limited system and an interference-limited system, respectively. For a noise-limited WLAN system, one important system performance metric is referred to as signal-to-noise-ratio (SNR), which must be lower than the protection ratio in a reliable wireless connection. If the received signal power is too close to the noise level, the wireless connection will be terminated, this situation is referred as an outage. The outage probability in noise-limited systems, without accounting the impact of interference, is expressed as [26]:

$$P_{out} = \frac{1}{2}\,\mathrm{erfc}[\frac{m - m_s}{\sqrt{2}\sigma}] \quad (4)$$

where σ is the signal strength standard deviation in dB; m is the average received signal power in dB; m_s is the receiver sensitivity in dB.

In a more general scenario, due to the working channel frequency fully or partially overlapping with another nearby transmission, the system is referred to as an interference-limited system [27]. This describes co-&adjacent-channel interference when the SNR is always stronger than the Rx sensitivity. In interference-limited WLAN systems the relevant performance metric is the signal-to-interference-ratio (SIR), which must be lower than the protection ratio in a reliable wireless connection, otherwise an outage occurs.

TABLE I: The Outage Probability Approximations Comparison

Actual Parameters			Wilk.	Sch.&Ye.	Chan	Exact
σ dB	τ_1 dB	τ_2 dB	$P^2_{out}\%$	$P^2_{out}\%$	$P^2_{out}\%$	$P^2_{out}\%$
3	5	5	34.1	34.2	32	34.1
3	5	10	18.6	18.4	18.5	18.4
3	10	20	1.1	1.0	1.2	1.1
6	10	10	23	23.7	20.5	23.6
6	10	20	13.3	13.4	12.9	13.4
6	20	20	2.2	2.1	2.3	2.2

Even though there is no practical means of predicting the exact received signal power or SIR, we can use a stochastic function to exactly measure the outage probability in the presence of interference, which was proposed in [28] and summarised by Sowerby in his Ph.D. thesis [29]. However, it could still be prohibitively computationally expensive to determine the outage probability in the presence of multiple interferers. To tackle this problem some approximate methods have been proposed in [30]–[32], which can dramatically decrease the computational cost in computing the outage probability. A performance comparison is drawn in Table I, in which the exact method [28], and three approximations proposed by Chan [30], Wilkinson [31] and Schwartz & Yeh [32] are investigated respectively. From the table we can see that every aforementioned approximation method can provide a very good result when σ is between 3 dB and 6 dB, which is a common occurring range in the metro environment [3].

In interest of computational efficiency in the presence of multiple interferers, in this paper we will employ Chan's method [30] to compute the outage probability. With n interferers and the corresponding power excess $(\tau_1, \tau_2, \ldots, \tau_n)$, Chan proposes an equivalent interfering signal τ_{eq} given by:

$$\tau_{eq} = -10 \times \log_{10}(\sum_{i=1}^{n} 10^{\frac{-\tau_i}{10}}) \quad (5)$$

and the power excess of the $i\text{-}th$ interferer τ_i is expressed as:

$$\tau_i = m - (m_i + R) \quad (6)$$

where m_i is the average power of the $i\text{-}th$ interferer at the receiver; R is the system minimally accepted SIR in dB, which is also known as the system protection ratio. Therefore, the outage probability in the presence of n interferers is

$$P_{out} = \frac{1}{2}\,\mathrm{erfc}[\tau_{eq}/2\sigma_{eq}] \quad (7)$$

where σ_{eq} equals the σ_{dB} of the desired signal. In interference-limited WLANs, the SIR is expressed as:

$$\mathrm{SIR}[\mathrm{dB}] = 10\log_{10}(E_b/I_0) + 10\log_{10}(f_b/B) \quad (8)$$

where E_b/I_0 is the energy per bit to co-channel interference power spectral density ratio; f_b is referred to as the channel data rate; B is referred to as the channel bandwidth. In planning the WLANs, SIR is a core criterion that needs to be considered carefully, because too low SIR will lead to a dramatically increased bit-error-rate (BER), which is unacceptable for DCS. As a function of E_b/I_0, for binary-frequency-shift keying (BFSK), BER is expressed as:

$$\mathrm{BER} = \frac{1}{2}\,\mathrm{erfc}(\sqrt{\frac{E_b}{2 \times I_0}}) \tag{9}$$

By integrating equation (8) and (9), the system protection ratio can be derived.

III. Methodology

A. System Modelling

In tunnel-based metro systems, there are two main types of architecture, namely section and station. Section is defined as the part between two adjacent stations. For the most part, the section area is an isolated two-way tunnel; the station is typically an underground building that has entrances and exits for trains going through. A typical station design drawing is shown in Figure 2. From this figure we can see that the track is divided into a station part and a section part, the partition boundaries denoted by K 25+737.8 and K 25+926.8 in Figure 2, respectively.

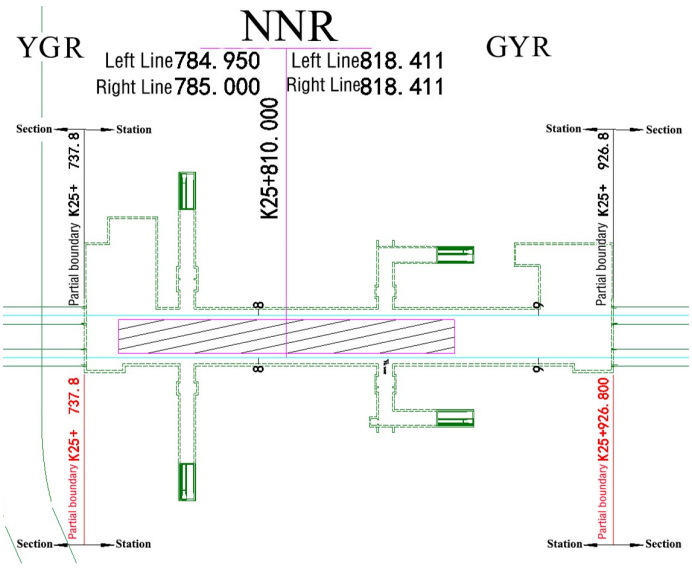

Fig. 2: The design drawing of Nanning Road Station (NNR)

The raidowave propagation behaviour in section and station is totally different. In the section, wireless propagation is mainly determined by the tunnel cross section shape and dimension and the tunnel curvature; on the other hand, in the station wireless propagation is much more complex and varied. From Figure 2 we can note that the station entrance and exit are connected to separated tunnels; when a train is running through the station entrance or exit, the line of sight (LOS) signal propagation between station and section will be to a great extent obstructed by the train, which can cause significant power reduction [3]. As a result, for a worst case scenario consideration, it is assumed that the section area and its neighboring station area are fully isolated, and that no radiowaves pass through. Therefore, in this paper, as it is difficult to characterize wireless transmission in stations (deterministically or stochastically), and the neighboring section and station are isolated, it is proposed that existing AP deployments are adopted and AP deployment optimization is only performed in the sections between stations.

In sections, it is assumed that the railway track is a continuous line, which means there are countless places where an AP can potentially be allocated. To render the problem tractable, the railway track is discretized into a number of subsections. At the joint between adjacent subsections there is a potential placement of an AP, and binary integers are used to show whether there is an AP placed in the joint or not. For a track discretized into $N-1$ subsections, the problem is formulated as:

$$\begin{cases} P_\mu = 1, & \text{AP is located} \\ P_\mu = 0, & \text{AP is not located} \\ \text{s.t.} \quad \mu \in 1, \ldots, N \end{cases} \tag{10}$$

where μ is the joint label. Consequently, a specific AP deployment is expressed by a particular value of the N long binary string $(P_1, \ldots, P_N)$. It follows that there exist $2^N - 1$ AP deployments. The set of all the AP deployments is denoted as Θ.

To determine a meaning full subsection length which yields a compromise between accuracy and tractability, we require knowledge of the correlation length of the shadowing fading in the tunnel. Within separations smaller than this length, the received signal will experience a typical (average) fade duration. It has been found in [3] and [33] that the correlation length range of shadowing varies significantly from 5 m to 300 m, which depends on the relevant dimensions of the signal propagation environment. In the case of tunnels we take a typical value for the subsection length is to be 60 m, which is consistent with reported shadow correlation lengths of a small number of 10s of meters in [18] and [34] .

B. Problem Formulation

In our prior work [20] a method to assess the feasibility and the overall performance of AP deployments has been established and successfully validated. In this method, we avoid a priori assumption on what constitutes a "nonsensical" deployment, all the AP deployment combinations are considered, the outage probability is utilized as the criterion to select the best deployments, the outage probability at each sampling point need to be assured as lower than the pre-specified threshold,

$$\begin{cases} P_{out\_i}(x) \leq R_{outage} \\ \quad \text{s.t.} \quad i \in 1, \ldots, I \end{cases} \tag{11}$$

where x is an AP deployment in Θ; P_{out_i} is the outage probability at sampling point i; I is the total number of sampling points; R_{outage} is the system outage probability

threshold. To render the system reliability in case of an AP failure, the outage probability threshold should still be satisfied when an AP is out of order,

$$P_{out\_i}(\dot{x}) \leq R_{outage} \tag{12}$$

where $\dot{x}$ is the AP deployment x with a faulty AP. The AP deployments which can simultaneously fulfill equation (11) and equation (12) are deemed feasible. All the feasible AP deployments form S. Additionally, we assume that the safety-critical operation is also achieved through hardware redundancy at each AP node.

In this paper, instead of using experience-based system optimisation factor to add preference on objectives in [20], the AP deployment optimization problem is formulated as:

$$\begin{cases} \min \ \ F(P^2_{out\_max}(x), P^2_{out\_mean}(x), H^2(x)) \\ \mathrm{s.t.} \ \ \mathrm{x} \in \mathrm{S} \subset \Theta \end{cases} \tag{13}$$

where $H(x)$ is the Hamming distance of the AP deployment x to a null AP deployment; P_{out_mean} is the mean value of the outage probability $\times 10^2$, $P_{out\_max}(x)$ is the max value of the outage probability the mean value of the outage probability $\times 10^3$. The aim of the optimisation is expressed as:

$$\tilde{\mathrm{x}} = \arg\min_{\mathrm{x} \in \mathrm{S}} F(x) \tag{14}$$

where $\tilde{x}$ is the optimal AP deployment.

C. Search Algorithm Application

After formulating the problem, we need to find an efficient search algorithm for the optimization result. In our prior work [20], we employed exhaustive search and experience-based system optimization factors, which achieved a good performance in a small-scale case study. However, some concerns arise if the brute-force exhaustive search method is applied to larger-scale AP deployments:

1) **Prohibitively high computational cost:** If we set the subsection length as 60 m, for a 2182 m track, there are 35 subsections. Through implementing the same methodology proposed in our prior work on a desktop (Intel i5-3570 3.4GHz, 8GB RAM), it needs 2088 days to evaluate all the 3.4×10^{10} AP deployments, which is almost infeasible.
2) **Optimsation result bias:** In our prior work [20], in order to covert multiple objectives into an overall objective, experience-based preference (e.g. system optimization factors) is predefined to each objective. However, when the system scale is large and the system is complex, due to there being insufficient knowledge and thorough analysis, this predefined preference is highly likely to be unreasonable, which can lead to an bias or even inaccurate optimisation result.

To relieve these concerns, we need a more advanced search algorithm that can not only search efficiently for the optimization result, but also has a guaranteed accuracy. Equation (13) dictates that we need to employ a multiple objective optimization programming (MOP). As the objective functions in a MOP problem are very likely to be contradictory, it will be difficult to have a solution that optimizes all the objectives simultaneously and the optimal result will be the solution that has the best tradeoff among these objectives.

To determine the best tradeoff efficiently, an advanced search algorithm MOEA/D [21] is customized, as it has been proven to be a good tool for solving MOP problems. In MOEA/D, the MOP problem $F(x)$ proposed in equation (13) is decomposed into M scalar optimization sub-problems by using the Techebycheff approach [36], so the cost function of the k^{th} sub-problem is expressed as:

$$g^{te}(x|\lambda^k, z^*) = \max_{1 \leq i \leq 3} (\lambda^k | f_i(x) - z_i^*) \tag{15}$$

where $f_1(x) = P^2_{out\_max}(x)$, $f_2(x) = P^2_{out\_mean}(x)$, $f_3(x) = H^2(x)$; g^{te} is the decomposition cost; λ^k is the weight vector; $z_i^* = (z_1^*, z_2^*, z_3^*)^{\mathrm{T}}$ is the reference vector, which is expressed as:

$$\begin{cases} z_1^* = \min(f_1(x) | x \in S) \\ z_2^* = \min(f_2(x) | x \in S) \\ z_3^* = \min(f_3(x) | x \in S) \end{cases} \tag{16}$$

By changing the weight vector λ in equation (15), different optima of the subproblem will be found. To provide sufficient and well spread optimum candidates, in MOEA/D the weight vector is uniformly spread. As the g^{te} is continuous with regard to λ, MOEA/D considers that if λ^k is close to λ^t, the optimum of the k^{th} sub-problem should be close to the optimum of the t^{th} sub-problem. Therefore, MOEA/D defines that the neighborhood of λ^k is formed by T closest (in terms of Euclidean distance) weight vectors in $(\lambda^1, \ldots, \lambda^M)^{\mathrm{T}}$, and the neighborhood of k^{th} sub-problem is formed by the sub-problems whose weight vectors are the neighbors of λ^k.

In each iteration, only the neighboring sub-problems are explored through using genetic algorithm (GA) [35], and the optimum of each sub-problem will be updated if a better one is found. When the maximum iteration number is reached, an external population (EP) will be outputted, which stores all the found non-dominated optima. These stored optima and EP are better known as Pareto optimal (PO) and Pareto front (PF) [36] respectively.

D. Decision Making

The optima stored in the EP are the optimal result candidates. As each member of the EP is non-dominated, this means there is no perfect among the EP such that the system designers need to define a dedicated trade-off by themselves. To define such a trade-off, the posterior preference must be specified. In some cases, if the system designers demand a more stable throughput in the train-to-wayside communication, the maximum outage probability should have more priority; in some protocols, i.e. the user datagram protocol (UDP), the mean outage probability is a privileged metric, because UDP is a best effort transmission, and lower mean outage probability leads to a higher cumulative throughput. Unlike the prior preferences (i.e. the predefined weight factors), adding posterior preference can provide a much broader solution space, which can bring an extra gain in planning AP deployment in DCS.

IV. Case Study

In Section II and Section III, the channel modelling and the optimisation methodology have been addressed, respectively. In this section, a real-world case study is presented to illustrate the efficacy of the proposed optimisation method.

A. System Environment

In this paper, we take Hefei Metro Line-I (HML-I) in China as a case study. HML-I is the first urban rail transit system in Hefei, the capital city of Anhui province in China. The construction of this metro line began in June 2012 and it was opened to the public at the end of 2016. HML-I has a length of 29.06 km and 23 stations, the whole metro system is operated in a tunnel environment and is fully managed by a WLAN-based CBTC system. A track layout is shown in Figure 3.

The detailed start distance kilometre (DK), end DK and length of each station and section in HML-I are listed in Table II. From this table we can find that there are 23 stations and 22 sections, where the longest station is Hefei Station which is 577 m long, the shortest station is Dadongmen Station at 147 m long, the longest section is between Huayuan Avenue Station and Jinxiu Avenue Station which is 2182 m long, the shortest section area is between Yungu Road Station and Naning Road Station which is 315 m long. As discussed in III-A, in this case study we will only implement the optimization in section areas.

TABLE II: Station List of the HML-I

Station				Section
Name	*From*	*To*	*Length* (m)	*Length* (m)
Hefei Sta. (HFS)	4K+306	4K+883	577	558
Fengyang Rd. Sta. (FYR)	5K+441	5K+628	187	551
Mingguang Rd. Sta. (MGR)	6K+179	6K+448	269	524
Dadongmeng Sta. (DDM)	6K+972	7K+119	147	739
Wuhu Rd. Sta. (WHR)	7K+858	8K+016	158	877
Nanyihuan Sta. (NYH)	8K+893	9K+099	206	1449
Taihu Rd. Sta. (THR)	10K+548	11K+010	462	476
Shuiyangjiang Rd. Sta. (SYJ)	11K+486	11K+685	199	799
Gedadian Sta. (GDD)	12K+484	12K+684	200	1428
Wanghucheng Rd. Sta. (WHR)	14K+112	14K+388	276	466
Gaotie Sta. (GTS)	14K+854	15K+120	266	633
Fanhua Ave. Sta. (FHA)	15K+753	15K+917	164	795
Dalian Rd. Sta. (DLR)	16K+712	17K+063	351	856
Huayuan Ave. Sta. (HYA)	17K+919	18K+114	195	2182
Jinxiu Ave. Sta. (JXA)	20K+296	20K+497	201	1353
Ziyun Rd. Sta. (ZYR)	21K+850	22K+018	168	849
Zhongshan Rd. Sta. (ZSR)	22K+867	23K+062	195	718
Fangxing Ave. Sta. (FXA)	23K+780	24K+047	267	906
Yungu Rd. Sta. (YGR)	24K+953	25K+422	469	315
Nanning Rd. Sta. (NNR)	25K+737	25K+926	189	582
Guiyang Rd. Sta. (GYR)	26K+508	26K+702	194	923
Hunan Rd. Sta. (HNR)	27K+625	27K+814	189	726
Huizhou Ave. Sta. (HZA)	28K+540	29K+010	470	0

TABLE III: Simulation Parameters

Network Parameters		Fading Parameters		
Parameters	*Value*	*Curvature Radius* [m]	*Pathloss Exponent*	*Std.* [dB]
Protocol	IEEE802.11	300	5.50	4.09
Frequency	2.4 GHz	350	5.47	4.23
Modu. Scheme	FHSS	380	5.45	4.32
Modu. Type	BFSK	450	5.40	4.52
Data Rate	1 MB/s	Straight	2	5
Chan. Bandwidth	3 MHz			
Chan. Hopping No.	25			
Trans. Scheme	CSMA/CA			
Trans. Power	15 dBm			
TX Gain	14 dBi			
RX Gain	12 dBi			
Proce. Gain	18 dB			
Rx Sensitive	-85 dBm			
R_{outage}	3.2 %			

B. Large-scale Fading Characteristics in Section Areas

The radiowave propagation behavior is variational in different dimensions of section. In this subsection, the parameters used for describing the large-scale fading characteristics in different types of section are discussed.

1) Straight Section: For the sake of simplifying the problem, we regard a track as straight when its curvature radius is greater than 600 m. In [37] and [38], it has been found that under an arched tunnel the radiowave will encounter around a 2 path-loss exponent and around 5 dB shadowing deviation. As the parameters were measured in a tunnel that has similar dimensions with the tunnel in HML-I, and was at a similar working frequency of 2.4 GHz, we will use these two proposed parameters to describe the radiowave propagation channel in this case study.

2) Curved Section: In this paper, we regard a track as curved when the curvature radius is less than 600 m. The large-scale fading characteristics in different types of curved railway tunnel at 2.4 GHz have been addressed in [18]. As the tunnel dimensions encountered are similar, we will use these addressed parameters to describe the large-scale fading characteristics in the curved tunnel of HML-I. The detailed fading parameters in this paper are shown in Table III. As the train is moving within different section types, the large-scale fading parameters will change, subject to the train's location.

C. Simulation Parameters

The key network parameters are defined in Table III. By referring to the DCS design requirements in HML-I, the acceptable BER must be lower than 10^{-6}, and based on equation (8) and (9), we can deduce the corresponding SIR threshold, which is 8.5 dB. In HML-I, the requirement on maximum latency is no more than 50 ms, and by following

Fig. 3: Track layout of HML-I

the derivation described in [20], we can deduce that the corresponding maximum accepted outage probability is 3.2%. As the IEEE-802.11 FHSS-based WLAN is used in the DCS of HML-I, there is a processing gain, in which the parameter of interest is the channel hopping number [39]:

$$\mathrm{G_p[dB]} = 10 \times \log_{10}(\mathrm{HN}) \tag{17}$$

where the HN is the hopping channel number. In HML-I, there are 25 hopping channels in DCS, as a result, the processing gain in data transmission is 14 dB.

D. Search Algorithm

The MOEA/D algorithm used to search the optimised AP deployments in HML-I is shown in **Algorithm 1**. The required input of this algorithm is given: The MOP function is equation (13); the iteration time it is set as 20; we will account $M = 500$ sub-problems, so that there will be 500 evenly spread weight vectors, namely $\lambda^1, \ldots, \lambda^{500}$; the neighborhood size is 75; the outage probability threshold is set as 0.032, therefore, O_t will be $(0.032 \times 100)^2$.

1) Initialize: After setting the input, some data are initialized. At the first step, it is necessary to find the T neighbors of each sub-problem by measuring the Euclidean distance between the accompanied weight vector. The index of these neighbors are stored in $L = (k_1, \ldots, k_M)^{\mathrm{T}}$. Then, randomly select AP deployments x_t as the initial population, where $x_t \in S$, $t = 1, \ldots, M$, and if $f_1(x_t) \leq O_t$ store the corresponding $F(x_t)$ as the CF_t, otherwise stores the $F(x_t)$ as ∞. Finally, based on experience, set the initial reference points $z^* = (z_1, z_2, z_3)$.

2) Update: For the t^{th} sub-problem, we will randomly chose two indexes ξ and θ from k_t, and use x_ξ and x_θ to generate an offspring y^t by using genetic operator. Then, to update the neighborhood, MOEA/D uses the g^{te} as the indicator to compare the $g^{te}(y^t|\lambda^t, z^*)$ with all the $g^{te}(x_i|\lambda^t, z^*)$, where $i \in k_t$. If $g^{te}(y^t|\lambda^t, z^*)$ is smaller than $g^{te}(x_i|\lambda^t, z^*)$ and $f_1(y^t) \leq O_t$, store the $CF_t = F(y^t)$ in EP if there is no member of that EP dominates it, and remove all the vectors dominated by $F(y^t)$. If $f_1(x_t) > O_t$, set $CF_t = \infty$. During this process, to update the reference points z^*, if $f_{ii}(y^t)$ is smaller z_{ii}, where $ii \in (1, 2, 3)$, update the z_{ii} with $f_{ii}(y^t)$.

3) Output: After 20 iterations, check whether every corresponding $[\mathrm{EP.Location}]$ fulfills the constraint stated in equation (12). Then output the eligible EP.

E. Result Search

After defining all the relative parameters and customizing the MOEA/D, in this part we search for the optimization result. As an indicative example, the search result for the section between FYR and HFS is shown in Figure 4. At the upper part of Figure 4, there is a 3D figure, and all of the four PO are marked by red dots. The X-axle, Y-axle and Z-axle represent $P_{out\_max}(x)$, $P_{out\_mean}(x)$ and $H(x)$ respectively. As all the PO have the same value on the Z-axle, for the sake of clarity, we cast the 3D figure to a 2D one. In this 2D figure, by fitting the four PO, we can get a solid line, which is referred to as the PF. This PF assumes an order of results which has only one objective better than the others.

The overall search result is shown in Table IV, where the section length, the radius of curvature of the section, AP candidates number, the spacing between two AP candidates, the PO AP deployments and the used AP number in the original planning are illustrated. We can see that the section with the most AP candidates is between JXA and HYA, in which 35 locations can be potentially placed an AP; the section with the least AP candidates is between NNR and YGR, only 6 locations are raised to potentially place an AP. To fulfil the users with different types of demands for each section, we select two PO from the Pareto set to display, namely minimized AP number preferred (when there are multiple options, chose the one with a lower mean value of outage probability) and minimized mean value of outage probability preferred. The used AP numbers in the original AP deployments are listed as a contrast. From the bottom line of Table IV we can see that the used AP numbers, for different preferred PO, are decreased by 21% and 13% respectively, which corresponds to a significant reduction in the overall system cost.

To verify the accuracy of the search result, we select a section (HZA to HNR) and compare the PF archived by brute force search (BFS) and MOEA/D. The comparison is shown in Figure 5. We can see that the result departure between BFS and MOEA/D is very small. Therefore, the accuracy of the MOEA/D is deemed to be very good indeed.

Algorithm 1: Search Algorithm

Initialize
set EP = [ ];
create M sub-problems;
generate M evenly spread weight vectors $(\lambda^1, \ldots, \lambda^M)^{\mathrm{T}}$;
find the T closest neighbors for each weight vector;
store the indexes of the T neighbors of each weight vector in $L = (k_1, \ldots, k_M)^{\mathrm{T}}$;
randomly pick M feasible solutions $x_1, \ldots, x_M$. For the t^{th} sub-problem, if $f_1(x_t) \leq O_t$, set the $CF_t = F(x_t)$, otherwise set $CF_t = \infty$, where $t(\in 1, \ldots, M)$;
set the initial reference points $z^* = (z_1, z_2, z_3)^{\mathrm{T}}$;
Update
for *it = 1, …, 20* **do**
  for $t = 1, \ldots, M$ **do**
    randomly chose two indexes ξ and θ from k_t;
    use x_ξ and x_θ as parents to generate offspring y^t;
    for *each index* $i \in k_t$ **do**
      if $g^{te}(y^t|\lambda^t, z^*) \leq g^{te}(x_i|\lambda^t, z^*) \&\& f_1(y^t) \leq O_t$ **then**
        $x_i = y^t$;
        $CF_t = F(y^t)$;
      else
        $CF_t = \infty$
      end
    for *each* $ii = 1, 2, 3$ **do**
      if $z_{ii} \geq f_{ii}(y^t)$ **then**
        $z_{ii} = f_{ii}(y^t)$
      end
    for *each* $CF_{iii} \in$ EP **do**
      while CF_t *is dominated by* CF_{iii} *= false* **do**
        add CF_t to EP;
        if CF_{iii} *is dominated by* CF_t *= true* **then**
          delate CF_{iii} from EP;
        end
      end
    end
  end
Return
for *each* $iiii = [\mathrm{EP.Location}]$ **do**
  if $f_1(\dot{x}_{iiii}) \geq O_t$ **then**
    delete EP
  end
Output EP;

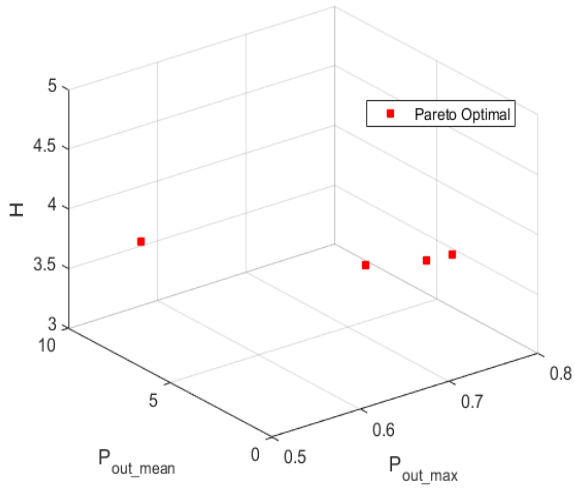

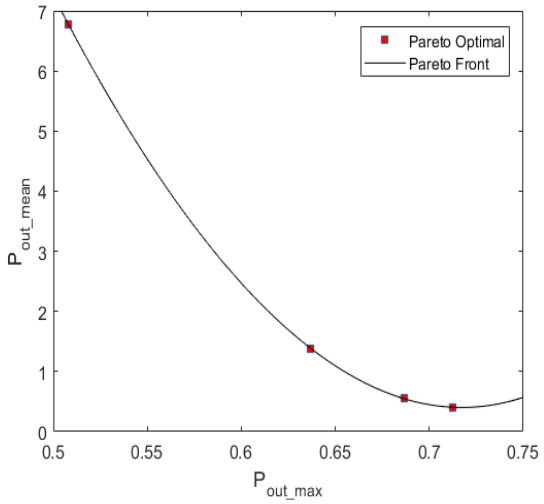

Fig. 4: Search result for the section between FYR to HFS

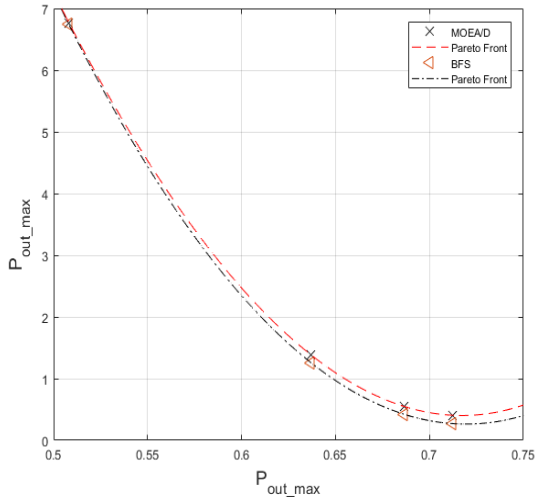

Fig. 5: The search result comparison between BFS and MOEA/D

V. Optimization Result Validation

In this section, we will validate the performance of the optimized AP deployment by comparing it to the original AP

TABLE IV: The Overall Optimisation Search Result

Section		*Length*	*R. of cur.*	*Candidate*	*Spacing*	*Pareto Optimal*		*AP No.*
From	To	(m)	(m)	Number	(m)	AP No. prefer.	Mean prefer.	Original
HZA	HNR	726	Straight	13	60	3-9	3-9	3
HNR	GYR	923	380	16	60	3-6-11	3-6-11	4
GYR	NNR	582	Straight	10	60	3-7	3-7	2
NNR	YGR	315	Straight	6	60	2-4	2-4	1
YGR	FXA	906	Straight	16	60	4-8-11	4-8-11	4
FXA	ZSR	718	Straight	13	60	5-10	5-10	4
ZSR	ZYR	849	Straight	15	60	5-8-12	5-8-12	3
ZYR	JXA	1353	Straight	24	60	3-10-12-16-24	3-10-12-16-24	5
JXA	HYA	2182	350/450	35	60	1-2-5-13-19-26-27-32-34	1-2-5-13-19-27-28-30-31-33	10
HYA	DLR	856	Straight	15	60	7-10	7-10	4
DLR	FHA	795	Straight	14	60	5-8	5-8	3
FHA	GTS	633	350	14	60	1-4-14	2-4-7-11	3
GTS	WHC	466	350	9	60	3-5	3-5	2
WHC	GDD	1428	350/450	25	60	2-12-15-20-22	2-3-5-6-8-12-16-22-25	8
GDD	SYJ	799	Straight	14	60	5-12	5-12	3
SYJ	THR	476	Straight	9	60	4-7	4-7	3
THR	NYH	1449	Straight	25	60	7-13-16-18-20	7-13-16-18-20	6
NYH	WHR	877	Straight	16	60	5-11-15	5-11-15	3
WHR	DDM	739	300	13	60	4-7-9	3-5-7-9	3
DDM	MGR	524	Straight	10	60	4-7	4-7	3
MGR	FYR	551	Straight	10	60	4-7	4-7	2
FYR	HFS	558	Straight	10	60	4-7	4-7	3
						66 (-21%)	73 (-13%)	84

planning. This validation will be conducted in the integrated simulation platform [1], [20].

A. Simulation platform

This integrated simulation platform is formed by two parts, one is the railway simulator BRaVE, and the other one is the network simulator OMNeT++.

1) Railway traffic simulator: BRaVE is a microscopic railway traffic simulator, developed by the Birmingham Centre for Railway Research and Education (BCRRE) at the University of Birmingham. BRaVE has a number of panels, including traffic, timetable, train run, train type, vehicle, infrastructure, station, routes, interlocking, junction, maps, models and rules. By configuring different panels, BRaVE can generate the railway traffic and simulate the functions of a railway control system.

2) Network simulator: OMNeT++ is an open source object-oriented modular discrete network simulation environment. To accurately validate the AP deployment in DCS, we should integrate OMNeT++ and BRaVE [40]. In this integrated simulation environment, the wireless data transmitted and received between the train and wayside APs in BRaVE will go through the real-world channel created in OMNeT++; meanwhile, the data transmission quality in BRaVE is determined in OMNet++ [1]. The data flow between OMNeT++ and BRAvE is shown in Figure 6.

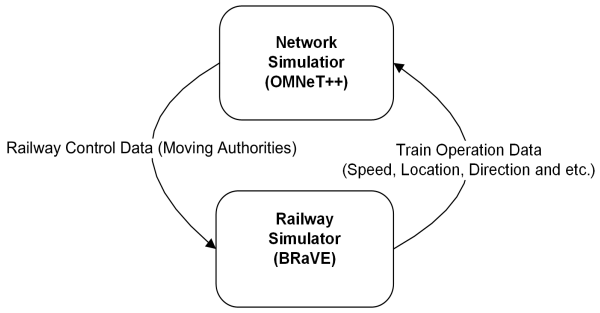

Fig. 6: The data flow in the integrated simulation platform

B. DCS performance validation

To prove the optimized AP deployments have a better performance than the original planning, the optimized and original AP deployments are simulated between DDM and FYR, and the simulation results are compared. The DK of the AP locations in the optimised AP deployment and the original AP deployment between DDM and FYR are specified in Table V. Firstly, the optimised AP deployment and the

TABLE V: The AP Deployment Between DDM and FYR

	DDM-MGR			MGR-FYR	
Original	K6+822	K6+662	K6+482	K6+008	K5+758
Optimised	K6+784	K6+604		K5+999	K5+640

original AP deployment in the section between DDM-FYR are configured in OMNeT++ respectively; the layout of these two AP deployments in OMNeT++ are displayed in Figure 7.

Then, a train service is set up in BRaVE. In this service, the train departs from DDM station, via MGR station, and arrives at FYR station. The whole journey takes 112 seconds. A screenshot of the simulation environment is shown in Figure 8. After finishing all the configurations in OMNeT++ andin BRaVE, the validation is started. The validation result is shown in Table VI.

From Table VI we can see that the optimised AP deployment has a greater mean and minimum signal-to-interference-plus-noise ratio (SNIR), a smaller mean and maximum BER, and a better packet error rate (PER), with a reduced AP number. Therefore, a conclusion is drawn that the optimised AP deployment is better than the original planning.

VI. Conclusion and Future Work

A well-planned AP deployment is vital for CBTC systems, in terms of system reliability and cost. In this paper, by customizing and adopting an accurate and more efficient search algorithm MOEA/D, the AP deployment optimization method proposed in our prior work has been consolidated and extended to be more practical. By using this extended optimization method, we optimized the AP deployment in HML-I, a real-world metro system. The relevant validation can prove that the optimized AP deployment can achieve a better data exchange performance than the original planning, meanwhile, the required AP number is decreased.

It is worthy mentioning that the methodology proposed in this paper is not just aiming to solve the AP planning problems in CBTC systems, but could be generic to all other types of radio-based train control systems with some minor customizations, such as the GSM-R based Europe Train Control Systems (ETCS) and the new generation Long Term Evolution for Railway (LTE-R) based train control systems. Moreover, the methodology can also be adapted to the planning work of the future 5G cellular systems and even the smart rail mobility designing. The relevant methodology applications will be extended in our future work.

(a)

(b)

Fig. 7: The AP deployment layouts in OMNeT++, a) the original deployment, b) the optimised deployment)

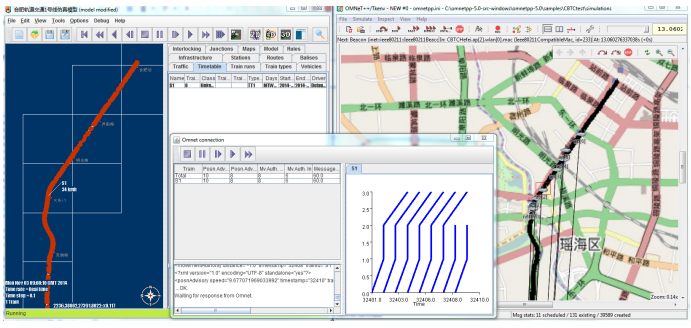

Fig. 8: The screenshot of the integrated simulation environment

References

[1] T. Wen, X. Lyu, D. Kirkwood, L, Chen, C. Constantinou and C. Roberts, "Co-simulation testing of data communication system supporting CBTC," *2015 IEEE 18th International Conference on Intelligent Transportation Systems*, Las Palmas, 2015, pp. 2665-2670.

[2] R. D. Pascoe and T. T. Eichorn, "What is communication-based train control?" *IEEE Vehicular Technology Magazine*, vol. 4, no. 4, pp. 16-21, Dec. 2009.

[3] K. Guan, Z. Zhong, J. I. Alonso and C. B. Rodriguez, "Measurement of distributed antenna systems at 2.4 GHz in a realistic subway tunnel environment," *IEEE Transactions on Vehicular Technology*, vol. 61, no. 2, pp. 834-837, Feb. 2012.

[4] H. Wang,F. R. Yu, L. Zhu, T. Tang and B. Ning, "Finite-state Markov modeling for wireless channels in tunnel communication-based train control systems," *IEEE Transactions on Intelligent Transportation Systems*, vol.15, no. 3, pp. 1083-1090, Jun. 2014.

[5] Beijing National Railway Research and Design Institute of Signal and Communication Co., Ltd.,"Railway GSM-R Mobile Communication System Engineering Evaluation Report," 2006.

[6] R. He, Z. Zhong, B. Ai and K. Guan. "Reducing the cost of high-speed railway communications: From the propagation channel view," *IEEE Transactions on Intelligent Transportation Systems*, vol. 16, no. 4, pp. 2050-2060, Aug. 2015.

[7] J. K. L. Wang, "Automatic planning and optimisation of in-building

TABLE VI: The Validation Result

	AP	Counts	mean:SNIR	min:SNIR	mean:BER	max:BER	PER
Optimised	7	7977	6.09×10^{10}	10.01	2.43×10^{-5}	1.9×10^{-1}	1.25×10^{-4}
Original	8	9086	2.94×10^{10}	0.46	8.49×10^{-5}	4.3×10^{-1}	2.20×10^{-4}

CDMA systems," Ph.D. thesis, The University of Auckland, Auckland, New Zealand, 2007.

[8] L. K. Pujji, K. W. Sowerby and M. J. Neve. "A new algorithm for efficient optimisation of base station placement in indoor wireless communication systems," *2009 7th Annual Communication Networks and Services Research Conference*, Moncton, 2009, pp. 425-427.

[9] L. K. Pujji, "Optimisation of base station placement for indoor wireless communications," Ph.D. thesis, The University of Auckland, Auckland, New Zealand, 2012.

[10] S. Namil, K. W. Sowerby and M. J. Neve "Are DS-CDMA indoor system deployments appropriate for OFDM networks?" *2012 Australian Communications Theory Workshop (AusCTW)*, Wellington, 2012, pp. 78-83.

[11] M. Kobayashi, S. Haruyama, R. Kohno and M. Nakagawa. "Optimal access point placement in simultaneous broadcast system using OFDM for indoor wireless LAN," *2000 IEEE 11th International Symposium on Personal, Indoor and Mobile Radio Communications*, London, 2000, pp. 200-204.

[12] N. Lu, N. Cheng, X. S. Shen, J. W. Mark and F. Bai, "Wi-Fi hotspot at signalized intersection: Cost-effectiveness for vehicular internet access," *IEEE Transactions on Vehicular Technology*, vol. 65, no. 5, pp. 3506-3518, May 2016.

[13] X. Du and K. Yang, "A map-assisted WiFi AP placement algorithm enabling mobile devices indoor positioning," *IEEE Systems Journal*, vol. PP, no. 99, pp. 1-9, Mar. 2016

[14] L. Wong, A. J. Mason, M. J. Neve and K. W. Sowerby, "Base station placement in indoor wireless systems using binary integer programming," *IEE Proceeding Communications*, vol. 153, no. 5, pp. 771-778, Oct. 2006.

[15] K. Guan, Z. Zhong, B. Ai and C. B. Rodriguez, "Modeling of the division point of different propagation mechanisms in the near-region within arched tunnels," *Wireless Personal Communications*, vol. 68, no. 3, pp. 489-505, Feb. 2013.

[16] R. He, Z. Zhong, B. Ai, J. Ding, Y. Yang and A. F. Molisch, "Short-term fading behavior in high-speed railway cutting scenario: Measurements, analysis, and statistical models," *IEEE Transactions on Antennas and Propagation*, vol. 61, no. 4, pp. 2209-2222, Apr. 2013.

[17] K. Guan,Z. Zhong, B. Ai, R. He, B. Chen, Y. Li and C. B. Rodriguez, "Complete propagation model in tunnels," *IEEE Antennas and Wireless Propagation Letters*, vol. 12, pp. 741-744, Jun. 2013.

[18] K. Guan, B. Ai, Z. Zhong, C. F. Lopez, L. Zhang, C. B. Rodriguez, A. Hrovat, B. Zhang, R. He and T. Tang "Measurements and analysis of large-scale fading characteristics in curved subway tunnels at 920 MHz, 2400 MHz, and 5705 MHz," *IEEE Transactions on Intelligent Transportation Systems*, vol. 16, no. 5, pp. 2393-2405, Oct. 2015.

[19] R. He, Z. Zhong, B. Ai, K. Guan, B. Chen, J. I. Alonso and C. B. Rodriguez, "Propagation channel measurements and analysis at 2.4 GHz in subway tunnels," *IET Microwaves, Antennas and Propagation*, vol. 7, no. 11, pp. 934-941, Aug. 2013.

[20] T. Wen, C. Constantinou, Z. Tian, L, Chen and C. Roberts, "Access point deployment optimization in CBTC data communication system," *IEEE Transactions on Intelligent Transportation Systems*, 2017. in press.

[21] Q. Zhang and H. Li, "MOEA/D: A multiobjective evolutionary algorithm based on decomposition," *IEEE Transactions on Evolutionary Computation*, vol. 11, no. 6, pp. 712-731, Dec. 2007.

[22] V. Erceg, K. V. S. Hari, M. S. Smith, D. S. Baum and *et al*, "Channel models for fixed wireless applications," Technical report, IEEE 802.16 Broadband Wireless Access Working Group, Jan. 2001

[23] A. Goldsmith, "Wireless communications," 1st ed. New York, NY: Cambridge University Press, 2005.

[24] V. Erceg, L. J. Greenstein, S. Y. Tjandra, S. R. Parkoff, A. Gupta, B. Kulic, A. A. Julius and R. Bianchi, "An empirically based path loss model for wireless channels in suburban environments," *IEEE Journal on Selected Areas in Communications*, vol.17, no.7, pp. 1205-1211, Jul. 1999.

[25] R. Prasad, "Effects of Rician faded and log-normal shadowed signals on spectrum efficiency in microcellular radio," *IEEE Transactions on Vehicular Technology*, vol.42, no. 3, pp. 274-281, Aug. 1993.

[26] W. C. Jakes, "Microwave mobile communications," New York, NY:John Wiley, 1974.

[27] K. Pahlavan, A. H. Levesque, "Wireless Information Networks," 2ed ed. Hoboken, NJ: Wiley-Interscience, 2005.

[28] Y. S. Yeh and S. C. Schwartz, "Outage probability in mobile telephony due to multiple log-normal interferers," *IEEE Transactions on Communication*, vol.COM-32, no. 4, pp. 380-387, Apr. 1984.

[29] K. W. Sowerby, "Outage probability in mobile radio systems," Ph.D. thesis, The University of Auckland, Auckland, New Zealand, 1989.

[30] G. K. Chan, "Design and analysis of a land mobile radio system under the effects of interference," Ph.D. thesis, The Carleton University, Ottawa, Canada, 1984.

[31] L.F. Fenton, "The sum of lognormal probability distributions in scatter transmission systems,"*IRE Transactions on Communications Systems*, vol.CS-8, no. 1, pp. 57-67, Mar. 1960.

[32] S. C. Schwartz and Y.S. Yeh, "On the distribution function and moments of power sums with log-normal components," *Bell System Technical Journal*, vol.61, no. 7, pp. 1441-1463, Sept. 1982.

[33] H. L. Bertoni,"Survey of observed characteristics of the propagation channel," in *Radio Propagation for Modern Wireless Systems*, 1st ed. Upper Saddle River, NJ:Prentice Hall, 1999.

[34] B. Ai, K. Guan, Z. Zhong, C. F. Lopez, L. Zhang, C. B. Rodriguez and R. He, "Measurement and analysis of extra propagation loss of tunnel curve," *IEEE Transactions on Vehicular Technology*, vol. 65, no. 4, pp. 1847-1858, Apr. 2016.

[35] M. Melanie, "An introduction to genetic algorithms," Cambridge, MA: MIT Press, 1996.

[36] K. Miettinen, "Nonlinear multiobjective optimization," Kluwer, MA: Norwell, 1999.

[37] J. M. Molina-Garcia-Pardo, M. Lienard, and P. Degauque, "Propagation in tunnels: Experimental investigations and channel modeling in a wide frequency band for MIMO applications," *EURASIP Journal on Wireless Communications and Networking - Special issue on advances in propagation modelling for wireless systems*, vol. 2009, no. 7, Mar. 2009

[38] M. S. Choi, D. S. Jo, J. G. Yook and H. K. P, "Path-loss characteristics in subway tunnel at 2.65 GHz, *Microwave and Optical Technology Letters*, vol. 48, no. 2, Feb. 2006.

[39] M. A. Abu-Rgheff, "Fundamentals of spread-spectrum techniques," in *Introduction to CDMA Wireless Communications*, Oxford, UK: Academic Press, 2007, pp. 153-194.

[40] A. Varga (2016) *Omnet++ Simulation Manual (5th ed.)*[Online]. Available: https://omnetpp.org/doc/omnetpp/manual/

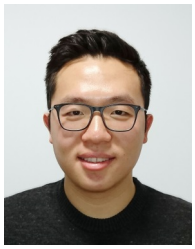

Tao Wen received his B.Eng degree in computer science from Hangzhou Dianzi University, Hangzhou, China, and MSc degree from University of Bristol, Bristol, UK, in 2011 and 2013, respectively. From 2013 to 2018, he is a PhD candidate at the Birmingham Centre for Railway Research and Education at the University of Birmingham, Birmingham, UK. His research interests include CBTC system optimization, railway signalling simulation, railway dependability improvement, wireless signal processing and digital filter research.

Costas Constantinou received the B.Eng. (Hons) degree in electronic and communications engineering and Ph.D. degree in electronic and electrical engineering from the University of Birmingham, Edgbaston, U.K., in 1987 and 1991, respectively. In 1989, he joined the Faculty of the School of Electronic and Electrical Engineering, University of Birmingham, and is now a Professor in Communications Engineering. He heads the radiowave propagation research activity in the communications engineering research group. He has been involved in the antennas and propagation research for body area communications led by Prof. Peter Hall since its inception in 2002 and is the PI on the latest EPSRC-funded effort to extend this research to the 60-GHz band. His research interests in communications span a broad range of topics that includes optics, electromagnetic theory, electromagnetic scattering and diffraction, electromagnetic measurement, radiowave propagation modeling, mobile radio, wireless networks, and future communications networks architectures.

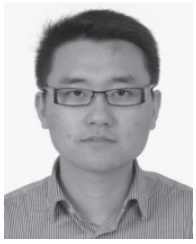

Lei Chen received the B.Eng. degree in automation engineering from Beijing Jiaotong University, Beijing, China, in 2005, and the Ph.D. degree in railway traffic management from the University of Birmingham, Birmingham, U.K., in 2012. He is currently a Birmingham Fellow for Railway Traffic Management with the Birmingham Centre for Railway Research and Education, University of Birmingham. His research interests include railway traffic management and control, railway safety critical system design, and railway simulation.

Zhu Li received the B.Eng. degree in electronic and electrical engineering from the University of Birmingham, Birmingham, U.K., in 2014 and the B.Eng. degree in telecommunication engineering from Huazhong University of Science and Technology, Wuhan, China. He is currently working toward the Ph.D. degree at the Birmingham Centre for Railway Research and Education, University of Birmingham. His research interests include energy -efficient train control and train automation in mainline railway , train trajectory optimization, and optimization techniques.

Clive Roberts is Professor of Railway Systems at the University of Birmingham. Clive is Director of the Birmingham Centre for Railway Research and Education, which is the largest railway research group in Europe with just over 100 researchers. He works extensively with the railway industry and academia in Britain and overseas. He leads a broad portfolio of research aimed at improving the performance of railway systems, including a leading a strategic partnership in the area of data integration with Network Rail. His main research interests lie in the areas of railway traffic management, condition monitoring, energy simulation and system integration.